A Graphical User Interface to compute the thermal and optical behaviour of metals of varying thicknesses under ultrashort laser pulse irradiation

Table of Contents

User guide for a computational tool to evaluate the thermal and optical behaviour of metals of varying thicknesses under ultrashort laser pulse irradiation

George Tsibidis

Institute of Electronic Structure and Laser (IESL), Foundation for Research and Technology (FORTH), Vassilika Vouton, 70013, Heraklion, Crete, Greece

Abstract

The employment of femtosecond pulsed lasers has received significant attention due to its capability to facilitate fabrication of precise patterns at the micro- and nano- lengths scales. A key issue for efficient material processing is the accurate determination of the thermal and optical parameters following irradiation of the solid with ultrashort laser pulses. More specifically, although numerous studies have examined laser conditions that induce thermal effects—yielding valuable insights into phenomena such as ablation, phase transitions, and material damage—the combined optical and thermal behaviour of thin films with thicknesses comparable to the optical penetration depth remains largely unexplored. Furthermore, the development of specialised computer algorithms or the use of expensive commercial software is often required for a detailed analysis which, further inhibits the efforts of the physics or material science communities to conduct a thorough investigation of the underlying physical phenomena.

The developed interface allows the evaluation of the impact of various parameters such as the photon energies, material thickness, pulse duration, pulse separation (in case of double pulses) and peak laser fluence on the thermal and optical effects t for various metals (Au, Ag, Cu, Al, Ni, Ti, Cr, Stainless Steel, W, Pt, Mo) and at three different substrates (Si, SiO_2 and soda lime silica glass). In addition, free standing films are, also, considered. A physical model based on the combined evaluation of the absorbed energy (i.e. via the calculation of the optical parameters of the stack) and the thermal effects (i.e. via the use of a Two Temperature Model) constitutes the underlying physical model.

1. Theoretical model

To describe the thermal effects on the material following irradiation with ultrashort laser pulses pulses, a theoretical framework is employed to explore the excitation and thermal response of a double-layered structure (thin metal film on a dielectric material). The simulation algorithm is based on the use of a Two Temperature Model (TTM) that represents the standard approach to evaluate the dynamics of electron excitation and relaxation processes in solids [1]. In this work, for the sake of simplicity, an 1D-TTM is used to describe the thermal effects due to heating of the thin films with laser pulses of wavelength λ_L for a pulse duration τ_p. It is noted that the solution of the TTM in 1D (along the energy propagation direction) is a standard approach used to describe thermal effects after irradiation of solids with femtosecond laser pulses [2, 3]. This is a reasonable choice assuming that, in principle, the laser spot radius is much larger (some tens of micrometers) than the thickness of the irradiated solid; therefore, the laser energy distribution along the lateral direction is considered uniform which means that the heat conduction along that direction is practically infinitesimal. Due to the presence of the substrate, the following set of rate equations is employed [4]

$$\begin{aligned}
C_e^{(m)}\frac{\partial T_e^{(m)}}{\partial t} &= \frac{\partial}{\partial z}\left(k_e^{(m)}\frac{\partial T_e^{(m)}}{\partial z}\right) - G_{eL}^{(m)}\left(T_e^{(m)} - T_L^{(m)}\right) + S^{(m)} \\
C_L^{(m)}\frac{\partial T_L^{(m)}}{\partial t} &= \frac{\partial}{\partial z}\left(k_L^{(m)}\frac{\partial T_L^{(m)}}{\partial z}\right) + G_{eL}^{(m)}\left(T_e^{(m)} - T_L^{(m)}\right) \\
C_e^{(S)}\frac{\partial T_e^{(S)}}{\partial t} &= \frac{\partial}{\partial z}\left(k_e^{(S)}\frac{\partial T_e^{(S)}}{\partial z}\right) - G_{eL}^{(S)}\left(T_e^{(S)} - T_L^{(S)}\right) + S^{(S)} \\
C_L^{(S)}\frac{\partial T_L^{(S)}}{\partial t} &= \frac{\partial}{\partial z}\left(k_L^{(S)}\frac{\partial T_L^{(S)}}{\partial z}\right) + G_{eL}^{(S)}\left(T_e^{(S)} - T_L^{(S)}\right)
\end{aligned} \tag{1}$$

where the subscript 'm' (or 'S') indicates the thin film (or substrate). In Eqs.1, $T_e^{(m)}$ and $T_L^{(m)}$ stand for the electron and lattice temperatures, respectively, of the upper layer. The thermophysical properties of the metal such as the electron $C_e^{(m)}$ (or lattice $C_L^{(m)}$) volumetric heat capacities, electron $k_e^{(m)}\left(=k_{e0}^{(m)}\frac{B_eT_e^{(m)}}{A_e\left(T_e^{(m)}\right)^2+B_eT_L^{(m)}}\right)$ heat conductivity, the electron-phonon coupling strengths $G_{eL}^{(m)}$, A_e, B_e and other model parameters that appear in the first two equations are listed in Table 1 (note A_g=194 Jm^{-3}K^{-1} for Cr). It is emphasised that as heat conduction in metals is, in principle, due to electrons, the thermal conductivity of the lattice is substantially smaller than that of the electron system. To include this large difference, $k_L^{(m)}$ is normally taken either equal to zero ($k_L^{(m)}$=0) [3, 5] or equal to a very small value compared to the electron heat conductivity ($k_L^{(m)}$=0.01$k_e^{(m)}$ is an expression that has been used in other reports [6, 7]). In this work and without loss of generality, we adopt the latter assumption.

The quantity $S^{(m)}$ represents the source term that accounts for the energy that the laser source provides to the metal surface which is sufficient to generate excited carriers on the thin film. As the purpose of the present investigation is to reveal the impact of optically excited *thin* films, it is important to take to into account the following processes: (i) a portion of the energy is absorbed from the material while part of the laser energy is transmitted into the substrate, (ii) the reflectivity and transmissivity of the irradiated material are influenced by a *multiple reflection process* between the two interfaces (air/metal and metal/substrate), (iii) the transmitted energy into the substrate is not sufficiently high to generate excited carriers and therefore, the third equation of Eqs.1 can be removed while the fourth can be simplified by $C_L^{(S)}\frac{\partial T_L^{(S)}}{\partial t}=\frac{\partial}{\partial z}\left(k_L^{(S)}\frac{\partial T_L^{(S)}}{\partial z}\right)+S^{(S)}$ where $T_L^{(S)}$, $C_L^{(S)}$, $k_L^{(S)}$stands for the substrate temperature, volumetric heat capacity and heat conductivity, respectively. The expression for the source term $S^{(m)}$ which is used to excite a metallic surface of thickness d is given from the following formula [5]

$$S^{(m)}=\frac{(1-R-T)\sqrt{4\log(2)}F}{\sqrt{\pi}\tau_p(\alpha^{-1}+L_b)}\exp\left(-4\log(2)\left(\frac{t-3t_p}{t_p}\right)^2\right)\frac{1}{(1-\exp(-d/(\alpha^{-1}+L_b))} \quad (2)$$

where R and T stand for the reflectivity and transmissivity, respectively, L_b corresponds to the ballistic length, α is the absorption coefficient that is wavelength dependent, and F is the peak fluence of the laser beam. The ballistic transport is also included in the expression as it has been demonstrated that it plays significant role in the response of the material [5]. Special attention is required for the ballistic length as in previous works, it has been reported that for bulk materials, L_b in *s/p*-band metals are comparable ($L_b^{(Au)}$=100 nm, $L_b^{(Ag)}$=142 nm, $L_b^{(Cu)}$=70 nm, $L_b^{(Al)}$=46 nm, $L_b^{(Mo)}$=20 nm [5]) while for the *d*-band metals such as Ni, Ti, Cr, stainless steelPt, W, it is of the same order as their optical penetration depth [5]. It is noted that the above values of the ballistic length were used for λ_L~ 400-500 nm pulses [5, 8]. The photon energy of the laser beam is expected to influence the ballistic length of the electrons [9] and therefore, the use of the above values for L_b at higher wavelengths (i.e. 1026 nm) could be questionable. Nevertheless, in the absence of appropriate values for L_b at higher photon energies in bibliography, the above values for the ballistic length are used.

The calculation of R and T and the absorbance $A=1-R-T$ are derived through the use of the multiple reflection theory [10]. Thus, the following expressions are employed to calculate the optical properties for a thin film on a substrate (for a *p*-polarised beam)

$$R=|r_{dl}|^2,\quad T=|t_{dl}|^2Re(\tilde{N}_S),\quad r_{dl}=\frac{r_{am}+r_{mS}e^{2\beta j}}{1+r_{am}+r_{mS}e^{2\beta j}},\quad t_{dl}=\frac{t_{am}t_{mS}e^{\beta j}}{1+r_{am}+r_{mS}e^{2\beta j}},\quad \beta=2\pi d/\lambda_L \quad (3)$$

$$r_{CD}=\frac{\tilde{N}_D-\tilde{N}_C}{\tilde{N}_D+\tilde{N}_C},\quad t_{CD}=\frac{2\tilde{N}_C}{\tilde{N}_D+\tilde{N}_C} \quad (4)$$

where the indices C=a,m and D=m,S characterise each material ('a', 'm', 'S' stand for 'air', 'metal', 'substrate', respectively). The complex refractive indices of the materials such as air, metal and substrate are denoted with $\tilde{N}_a=1$, $\tilde{N}_m=Re(\tilde{N}_m)+Im(\tilde{N}_m)j$, $\tilde{N}_S=Re(\tilde{N}_m)+Im(\tilde{N}_m)j$. It is noted that a Drude-Lorentz model is used to obtain the dielectric function for each metal based on the analysis by Rakic *et* al. (where both interband and intraband transitions are assumed) [11]. As the optical parameters of an excited material does not remain constant during the excitation process [12], to introduce the transient change, a temporally varying expression of the dielectric function is provided by including a temperature dependence on the reciprocal of the electron relaxation time τ_e (i.e. $\tau_e=\left[A_e\left(T_e^{(m)}\right)^2+B_eT_L^{(m)}\right]^{-1}$) [13]. The values of the refractive indices of the metals in this study (at 300 K are given in Table 1).

The set of equations Eqs.1-4 are solved by using an iterative Crank-Nicolson scheme based on a finite-difference method. It is assumed that the system is in thermal equilibrium at t=0 and, therefore, $T_e^{(m)}(z,t=0)$=$T_L^{(m)}(z,t=0)=300$ K. A thick substrate is considered (i.e. $k_L^{(S)}\frac{\partial T_L^{(S)}}{\partial z}=0$) while adiabatic conditions are applied on the surface of the metallic surface (i.e. $k_e^{(m)}\frac{\partial T_e^{(m)}}{\partial z}=0$). Finally,

the following boundary conditions are considered on the interface between the top layer and the substrate: $k_L^{(m)} \frac{\partial T_L^{(m)}}{\partial z} = k_L^{(S)} \frac{\partial T_L^{(S)}}{\partial z}, k_e^{(m)} \frac{\partial T_e^{(m)}}{\partial z} = 0, T_L^{(m)} = T_L^{(S)}$.

	Metal										
Parameter	**Au**	**Ag**	**Cu**	**Al**	**Ni**	**Ti**	**Cr**	**Steel (100Cr6)**	**W**	**Mo**	**Pt**
$\widetilde{N}_m$	DL [11]	DL [11]	DL [11]	DL [11]	DL [11]	DL [11]	DL [11]	DL [13]	DL [11]	- [11]	DL [11]
$G_{eL}^{(m)}$ [$Wm^{-3}K^{-1}$]	Ab-Initio [14]	Ab-Initio [14]	Ab-Initio [14]	Ab-Initio [14]	Ab-Initio [14]	Ab-Initio [14]	42×10^{16} [5]	Ab-Initio [15]	Ab-Initio [14]	Ab-Initio [14]	Ab-Initio [14]
$C_e^{(m)}$ [$Jm^{-3}K^{-1}$]	Ab-Initio [14]	Ab-Initio [14]	Ab-Initio [14]	Ab-Initio [14]	Ab-Initio [14]	Ab-Initio [14]	$A_g T_e^{(m)}$ [5]	Ab-Initio [15]	Ab-Initio [14]	Ab-Initio [14]	Ab-Initio [14]
$C_L^{(m)}$ [$\times10^6\ Jm^{-3}K^{-1}$]	2.48 [5]	2.5 [7]	3.3 [5]	2.4 [16]	4.3 [5]	2.35 [17]	3.3 [5]	3.27 [15]	2.5 [17]	2.33 [5]	2.8 [15]
$k_{e0}^{(m)}$ [$Wm^{-1}K^{-1}$]	318 [5]	428 [7]	401 [5]	235 [16]	90 [5]	21.9 [17]	93.9 [5]	46.6 [15]	21.9 [17]	138 [5]	72 [15]
A_e [$\times10^7\ s^{-1}K^{-2}$]	1.18 [7]	0.932 [7]	1.28 [7]	0.376 [16]	0.59 [7]	1 [17]	7.9 [6]	0.98 [15]	1 [17]	1 [6]	1 [15]
B_e [$\times10^{11}\ s^{-1}K^{-1}$]	1.25 [7]	1.02 [7]	1.23 [7]	3.9 [16]	1.4 [7]	1.5 [17]	13.4 [6]	2.8 [15]	1.5 [17]	1.5 [6]	1.5 [15]
T_{melt} [K]	1337 [18]	1234 [18]	1357 [18]	933 [18]	1728 [18]	1941 [18]	2180 [18]	1811 [18]	1941 [18]	2896 [18]	2045 [18]

Table 1: Optical and thermophysical properties of materials (*DL* stands for Drude-Lorentz model).

It has to be emphasised that a more rigorous approach would also require the investigation of the impact of the electron (in the metal) – phonon (in the dielectric) scattering (EM-PD) heat transfer across metal-dielectric surfaces. More specifically, in previous reports, it has been shown that, especially for very thin films, the impact of EM-PD coupling increases at decreasing thicknesses and this phenomenon leads to remarkable variation in the relaxation process [19]. Thus, special emphasis on the role of the thermal resistance (related to the reciprocal of the EM-PD coupling) should be given. Nevertheless, in those studies, the use of approximate expressions both for the thermophysical and the optical parameters of the irradiated metals as well as the neglect of the relation of the optical parameters variation with thickness (i.e. application of the multiple reflection theory) do not allow a direct and consistent interpretation with experimental data. Furthermore, in those studies, a fitting approach through the use of appropriate experimental protocols was performed to estimate the thermal resistance. Thus, despite a non-vanishing EM-PD coupling, the evaluation of the associated thermal resistance is not straightforward. In this study, the incorporation of the role of thermal resistance on the thermal effects on the irradiated material has not been used; however, the evaluation of the damage threshold and comparison with experimental data are expected to function as a test for the need of a more complex (but, anyway, more consistent with the application of all underlying physical mechanisms).

2. Steps to perform the evaluation of the thermal phenomena and optical parameters via the interface

In order to use the computational tool, the user has to select, firstly,

a) the laser conditions (i.e. laser wavelength, pulse duration, pulse delay (in case of double pulses), laser peak fluence)
b) metal (type of metal and thickness)
c) substrate.

a) the ‘laser wavelength’ must be edited in ‘nm’.
The ‘pulse duration’ (Full Width at Half Maximum of a Gaussian-like pulse) must be edited in ‘fs’.

The ‘pulse delay’ (time separation between subsequent pulses) must be edited in ‘fs’.
The value in ‘Time-interval end (ps)’ (The maximum time t_{max} within the interval [0, t_{max}], over which the evolution of the optical and thermal effects is assessed) must be edited in ‘ps’.
The ‘thickness of material’ (thickness of the metal) must be edited in ‘nm’.
The ‘Laser Peak fluence’ must be edited in ‘J/cm^2’.

b) Calculations are currently performed for the class ‘metal’: ‘Au’, ‘Ag’, ‘Cu’, ‘Al’, ‘Ni’, ‘Cr’, ‘Ti’, ‘Steel’ (100Cr6), ‘W’, ‘Mo’, ‘Pt’.

c) Four types of materials are considered as ‘Substrate’: ‘Silicon’, ‘Fused Silica’, ‘Soda Lime Silica Glass’, ‘Air’.

3. Methodology

The algorithm's execution considers both the thermophysical and optical parameters of the irradiated metal/substrate complex. The selection of the materials was based on considering the most common metals and substrates while it is aimed to be extended soon to other metals and configurations (multi-layered materials, etc). Similarly, an upcoming code update will enable users to study the dynamics of wide-bandgap materials, including semiconductors, oxides, dielectrics, and polymers.

A minimal intervention is required from the user, mostly, to introduce the refractive index and extinction coefficient for some materials.

4. Input/Output

i. Range of the input variables

- For the ‘pulse duration’ (τ_p), faster solutions are obtained for values between 100 fs (where the TTM is valid) and up to some hundreds of ps (or few ns). Execution of the code is more time consuming for longer pulses. In principle, the code was derived especially, to illustrate thermal and optical effects for ultrashort pulses. Although the code, in effect can be used for ‘ns’ long pulses, despite the long execution time, a significantly faster code is planned to be incorporated soon to address phenomena at the ns-scale.
- For the ‘pulse delay’ (t_{delay}), faster solutions are obtained for values between 0 fs (single pulse) and up to some hundreds of ps. Pulse delays in the ns scale could also be tried. It might take longer to run.
- For the ‘Time-interval end (ps)’ This value is the end of the interval within which the dynamics of various parameters are evaluated. As a general guideline, the following expression can be used for the estimate of this value to obtain a clear representation of the parameter dynamics (for delayed pulses): $(12^* \tau_p + t_{delay} + 80000)/1000$. By contrast, if the time delay is zero, then, the expression $6^* \tau_p + 40000)/1000$ is used. It is noted the value is not restrictive. The recommended value is a typical value which illustrates the relaxation time range. Of course, shorter values or longer values can, also, be selected. For example, irradiation with a double pulse, i.e. 170 fs for each pulse while the pulse separation is 2 ps, a representative value for ‘Time-interval end (ps)’ could be ~100 ps. Longer values can be used but depending on the pulse duration and pulse separation (in case of double pulses), more execution time might be required while the actual dynamics during the initial stages will not be illustrated in the figures (however, an analysis of the data files will allow a closer look in ‘user defined’ region).
- For the ‘thickness of material’, values between ~10-15 nm (marginally lower than the optical penetration depth) and <~1 μm (in principle, some hundreds of nm where the metal starts to behave as a bulk solid).
- For the ‘Laser Peak fluence’, values below 1 J/cm^2 (reasonable values of for metals) should be, generally, used at wavelengths (<1300 nm) and films thicker than 30-40 nm. Certainly, the type of the material, also, plays an important role. Larger values can also be used to investigate more extreme conditions (ablation conditions) or electron dynamics at smaller photon energies (corresponding to wavelengths >1.5 μm). It is emphasised, though, that if the laser conditions lead to extremely high electron temperatures (>50000 K), the analysis becomes problematic; this is due to the fact that the thermophysical properties of the irradiated metal were obtained from Ref.[14] which assumed the production of less energetic electrons. In that case, an alternative investigation is required and therefore, the execution of the code stops (see below, and discussion on Figure 2). Thus, the ‘allowed value’ Laser Peak fluence should, simply, not lead to electron temperatures >50000 K. The code is scheduled to be updated to consider higher-energy electrons.
- For the ‘laser wavelength’, the range of the wavelength values of the laser beam that irradiates the metal is taken on data from paper of Rakic et al [11] (see also range in RefractiveIndex.INFO - Refractive index database considering

the choice 'Rakic…'. In general, the wavelength range that has been tested so far for the purposes of this interface lie between 248 nm and up to some micrometers.

IMPORTANT:

- ✓ for 'Steel', for one wavelength ('1026 nm'), the optical properties of the material have already been incorporated into the model and no intervention from the user is required. For other laser wavelengths, the user has to enter: 'the real part of the refractive index' and the 'imaginary part of the refractive index (extinction coefficient)'.
- ✓ Similarly, for 'Mo', for one wavelength ('1026 nm'), the optical properties of the material have already been incorporated into the model and no intervention from the user is required. For other laser wavelengths, the user has to enter: 'the real part of the refractive index' and the 'imaginary part of the refractive index (extinction coefficient)'. Data should be collected from either the above database or from any other source.
- ✓ For 'Silicon' substrate, for four wavelengths ('248 nm', '515 nm', '800 nm', '1026 nm') the refractive index of the substrate has already been incorporated and no intervention from the user is required. For other laser wavelengths, the user has to enter: 'the real part of the refractive index' and the 'imaginary part of the refractive index (extinction coefficient)'. Data should be collected from either the above database or from any other source.
- ✓ Other substrates that are used in this interface are 'SiO_2', 'Soda Lime glass', 'Air' (i.e. free standing film). The refractive indices for those substrates are taken from the above database automatically.

ii. Execution of the Code

Following entering the above data, the user has to press the button 'Calculate' in order to start the evaluation of the evolution of the temperatures of the electrons, lattice and optical parameters inside the irradiated material as well as the impact of the substrate.

iii. Output

The execution of the code leads firstly to the creation of a directory named after the metal that has been selected (for example: 'Cr'). Inside the directory, a series of figures (in .png format) are produced. To facilitate data management and enable further analysis, the text files (.txt format) used to generate the figures are also provided. Finally, a file (in .txt format) that summarises the conditions is also produced. Below, an example for a test material ('Cr') is illustrated:

Material: Cr
Substrate: SiO_2
Thickness of First Layer (m) = 5.000000e-08
Thickness of Substrate (m) = 1.000000e-07
Pulse delay (s) = 0
Wavelength (m) = 1.026000e-06
Fluence (J/cm^2) = 1.000000e-01

Figure Files

- 'Reflectivity.png': The evolution of the reflectivity of the stack is illustrated in Fig.1a (*red line*). The *black dashed line* shows the evolution of the laser intensity (in arbitrary units).
- 'Transmissivity.png': The evolution of the transmissivity of the stack is illustrated in Fig.1b (*red line*). The *black dashed line* shows the evolution of the laser intensity (in arbitrary units).
- 'Absorptivity.png': The evolution of the absorptivity of the stack is illustrated in Fig.1c (*red line*). The *black dashed line* shows the evolution of the laser intensity (in arbitrary units).
- 'Te_Tl_t.png': The evolution of the electron temperature T_e (*red line*) and the lattice temperature T_L (*blue line*) on the surface of the metal is illustrated in Fig.1d. The *black dashed line* shows the evolution of the laser intensity (in arbitrary units).
- 'Te_t_z.png': The evolution of the electron temperature T_e inside the metal's volume is illustrated in Fig.1e.
- 'TL_t_z_stack.png': The evolution of the lattice temperature T_L inside the stack's (metal/substrate) volume is illustrated in Fig.1f. The *white dashed line* defines the interface between the metal and the substrate.
- 'TL_t_z_upper.png': The evolution of the lattice temperature T_L inside the metal's volume is illustrated in Fig.1g.
- 'TL_t_z_upper_layer_contour.png': The evolution of the lattice temperature T_L inside the metal's volume is illustrated in Fig.1h. Contours are included in the figure that shows the isotherms.

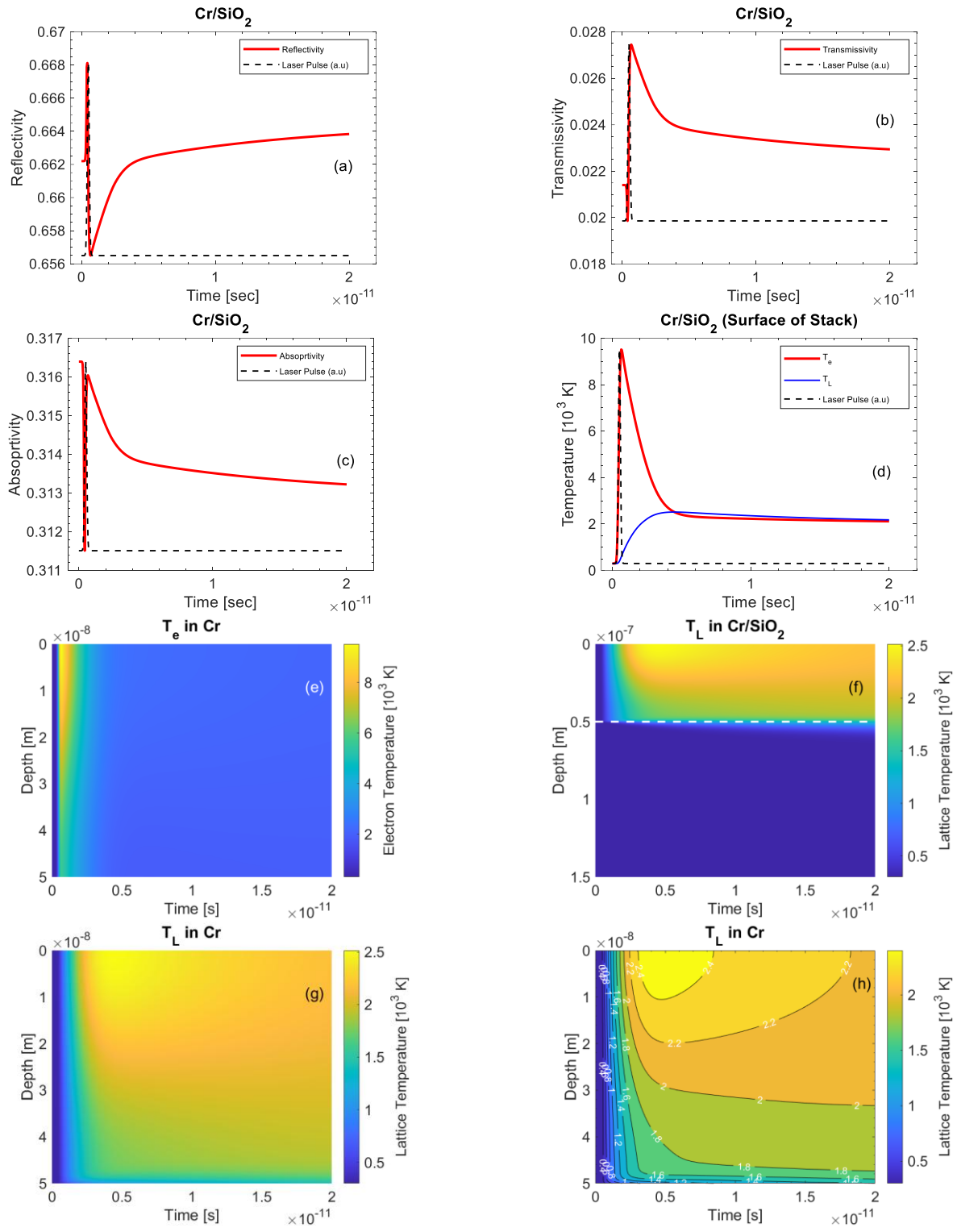

Figure 1: Evolution of (a) Reflectivity, (b) Transmissivity, (c) Absorptivity. (d) Electron Temperature and lattice temperature evolution, (e) Electron temperature evolution inside the depth of Cr. Lattice temperature evolution inside the stack (f), metal (g). (h) Contour plot of the Lattice temperature evolution inside the metal (lines show the isotherms).

Text Files

- 'Stack depth_(m).txt': A column that indicates the stack thickness in discretized form.

- 'Metal depth_(m).txt': A column that indicates the metal thickness in discretized form.
- 'Time_Intensity_reflectivity.txt': A three column matrix providing the 'Time', 'Intensity' (Arbitrary Units), 'Reflectivity'.
- 'Time_Intensity_tranmissivity.txt': A three column matrix providing the 'Time', 'Intensity' (Arbitrary Units), 'Transmissivity'.
- 'Time_Intensity_absorptivity.txt': A three column matrix providing the 'Time', 'Intensity' (Arbitrary Units), 'Absorptivity'.
- 'Time_Intensity.txt': A two column matrix providing the 'Time', 'Intensity' (Arbitrary Units).
- 'Te_upper_layer_(t,z)_(K).txt': A matrix that provides the T_e field inside the metal (rows and columns correspond to the depth and time, respectively).
- 'TL_stack_(t,z)_(K).txt': A matrix that provides the T_L field inside the stack (rows and columns correspond to the depth and time, respectively).
- 'TL_upper_layer_(t,z)_(K).txt': A matrix that provides the T_L field inside the metal (rows and columns correspond to the depth and time, respectively).
- 'Time_Te_TL.txt': A three column matrix giving the 'Time', 'T_e', 'T_L'.
- 'Conditions_materials_results.txt': The text file that is produced provides a summary of the laser conditions and material parameters and it can have the following content:

Case 1: Conditions above the melting point.

Material: Cr
Substrate: SiO2
Thickness of First Layer (m) = 5.000000e-08
Thickness of Substrate (m) = 1.000000e-07
Pulse delay (s) = 0
Wavelength (m) = 1.026000e-06
Fluence (J/cm2) = 1.000000e-01
Maximum Temperature on surface (K) = 2.514741e+03
Melting Temperature (T_melt) (K) = 2180
Thickness of Molten material (i.e. if Lattice Temperature in the layer is larger than Tmelt) (m) = 2.050000e-08
Ablation Temperature (T_ablation) (K) = 2.796800e+03

Case 2: Conditions above the ablation threshold.

Material: Cr
Substrate: SiO2
Thickness of First Layer (m) = 5.000000e-08
Thickness of Substrate (m) = 1.000000e-07
Pulse delay (s) = 0
Wavelength (m) = 1.026000e-06
Fluence (J/cm2) = 1.500000e-01
Maximum Temperature on surface (K) = 3.592502e+03
Melting Temperature (T_melt) (K) = 2180
Thickness of Molten material (i.e. if Lattice Temperature in the layer is larger than Tmelt) (m) = 4.900000e-08
Ablation Temperature (T_ablation) (K) = 2.796800e+03
Thickness of ablated material (i.e. if Lattice Temperature in the layer is larger than Tcritical) (m) = 2.800000e-08

Case 3: Conditions leading to T_e larger than 50000 K and thermophysical are not well characterised. Calculations do not finish at maximum time (see Figure 2).

Material: Cr
Substrate: SiO2
Thickness of First Layer (m) = 5.000000e-08
Thickness of Substrate (m) = 1.000000e-07
Pulse delay (s) = 0
Wavelength (m) = 1.026000e-06
Fluence (J/cm2) = 3
Maximum Temperature on surface (K) = 1.356400e+03
Melting Temperature (T_melt) (K) = 2180
Ablation Temperature (T_ablation) (K) = 2.796800e+03

COMMENT
Code stopped at a time before the Electron Temperature (Te) exceeded 50000 K.
This is due to the fact that the thermophysical properties are not well characterised above this value. Try a lower fluence.

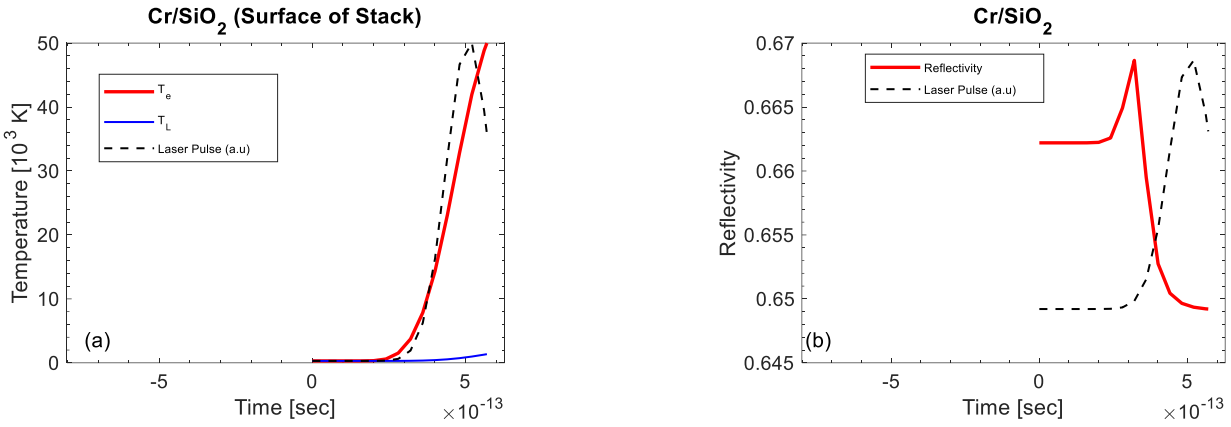

Figure 2: Evolution of (a) Electron Temperature and lattice temperature (b) Reflectivity.

Further assistance

For more information on the theoretical model read Refs.[20-22] or contact George D. Tsibidis (Institute of Electronic Structure and Laser-) at tsibidis@iesl.forth.gr. Furthermore, it is noted that a complimentary module of the code has been developed to evaluate the damage thresholds (i.e. minimum laser peak fluence that leads to material melting). This module is on NFFA Tool.

5. References

[1] S.I. Anisimov, B.L. Kapeliovich, T.L. Perel'man, Electron-emission from surface of metals induced by ultrashort laser pulses, Zhurnal Eksperimentalnoi Teor. Fiz. 66(2) (1974 [Sov. Phys. Tech. Phys. 11, 945 (1967)]) 776-781.
[2] A. Rämer, O. Osmani, B. Rethfeld, Laser damage in silicon: Energy absorption, relaxation, and transport, Journal of Applied Physics 116(5) (2014) 053508.
[3] J.K. Chen, J.E. Beraun, Modelling of ultrashort laser ablation of gold films in vacuum, J Opt a-Pure Appl Op 5(3) (2003) 168-173.
[4] B. Gaković, G.D. Tsibidis, E. Skoulas, S.M. Petrović, B. Vasić, E. Stratakis, Partial ablation of Ti/Al nano-layer thin film by single femtosecond laser pulse, Journal of Applied Physics 122(22) (2017) 223106.
[5] J. Hohlfeld, S.S. Wellershoff, J. Güdde, U. Conrad, V. Jahnke, E. Matthias, Electron and lattice dynamics following optical excitation of metals, Chemical Physics 251(1-3) (2000) 237-258.
[6] A.M. Chen, L.Z. Sui, Y. Shi, Y.F. Jiang, D.P. Yang, H. Liu, M.X. Jin, D.J. Ding, Ultrafast investigation of electron dynamics in the gold-coated two-layer metal films, Thin Solid Films 529 (2013) 209-216.
[7] A.M. Chen, H.F. Xu, Y.F. Jiang, L.Z. Sui, D.J. Ding, H. Liu, M.X. Jin, Modeling of femtosecond laser damage threshold on the two-layer metal films, Applied Surface Science 257(5) (2010) 1678-1683.
[8] S.S. Wellershoff, J. Hohlfeld, J. Güdde, E. Matthias, The role of electron–phonon coupling in femtosecond laser damage of metals, Applied Physics A 69(1) (1999) S99-S107.
[9] J. Byskov-Nielsen, J.M. Savolainen, M.S. Christensen, P. Balling, Ultra-short pulse laser ablation of copper, silver and tungsten: experimental data and two-temperature model simulations, Applied Physics a-Materials Science & Processing 103(2) (2011) 447-453.
[10] M. Born, E. Wolf, Principles of optics : electromagnetic theory of propagation, interference and diffraction of light, 7th expanded ed., Cambridge University Press, Cambridge ; New York, 1999.
[11] A.D. Rakic, A.B. Djurisic, J.M. Elazar, M.L. Majewski, Optical Properties of Metallic Films for Vertical-Cavity Optoelectronic Devices, Applied Optics 37(22) (1998) 5271-5283.
[12] E. Bevillon, R. Stoian, J.P. Colombier, Nonequilibrium optical properties of transition metals upon ultrafast electron heating, Journal of Physics-Condensed Matter 30(38) (2018) 385401.
[13] G.D. Tsibidis, A. Mimidis, E. Skoulas, S.V. Kirner, J. Krüger, J. Bonse, E. Stratakis, Modelling periodic structure formation on 100Cr6 steel after irradiation with femtosecond-pulsed laser beams, Applied Physics A 124(1) (2017) 27.
[14] Z. Lin, L.V. Zhigilei, V. Celli, Electron-phonon coupling and electron heat capacity of metals under conditions of strong electron-phonon nonequilibrium, Physical Review B 77(7) (2008) 075133.
[15] F. Fraggelakis, G.D. Tsibidis, E. Stratakis, Tailoring submicrometer periodic surface structures via ultrashort pulsed direct laser interference patterning, Physical Review B 103(5) (2021) 054105.
[16] B.H. Christensen, K. Vestentoft, P. Balling, Short-pulse ablation rates and the two-temperature model, Applied Surface Science 253(15) (2007) 6347-6352.
[17] S. Petrovic, G.D. Tsibidis, A. Kovacevic, N. Bozinovic, D. Perusko, A. Mimidis, A. Manousaki, E. Stratakis, Effects of static and dynamic femtosecond laser modifications of Ti/Zr multilayer thin films, Eur Phys J D 75(12) (2021) 304.

[18] D.R. Lide, CRC Handbook of Chemistry and Physics, 84th Edition, 2003-2004).
[19] L. Guo, S.L. Hodson, T.S. Fisher, X.F. Xu, Heat Transfer Across Metal-Dielectric Interfaces During Ultrafast-Laser Heating, Journal of Heat Transfer-Transactions of the Asme 134(4) (2012).
[20] G.D. Tsibidis, E. Stratakis, Impact of substrate on opto-thermal response of thin metallic targets under irradiation with femtosecond laser pulses, J Cent South Univ 29(10) (2022) 3410-3421.
[21] G.D. Tsibidis, D. Mansour, E. Stratakis, Damage threshold evaluation of thin metallic films exposed to femtosecond laser pulses: The role of material thickness, Opt Laser Technol 156 (2022) 108484.
[22] G.D. Tsibidis, E. Stratakis, Tailoring the ultrafast dynamics and electromagnetic surface modes on silicon upon irradiation with mid-infrared femtosecond laser pulses using ${\mathrm{SiO}}_{2}$ coatings, Physical Review B 109(18) (2024) 184113.